Journal of Materials Chemistry C

Efficient orange-red phosphorescent organic light-emitting diode using in situ synthesized copper(I) complex as the emitter

Journal:	*Journal of Materials Chemistry C*
Manuscript ID:	TC-ART-03-2014-000410.R2
Article Type:	Paper
Date Submitted by the Author:	23-May-2014

Complete List of Authors:	Wei, Feng; Inner Mongolia University, College of Chemistry and Chemical Engineering; Peking University, College of Chemistry and Molecular Engineering Qiu, Jacky; University of Toronto, Liu, Xiaochen; Peking University,, College of Chemistry and Molecular Engineering Wang, Jian-Qiang; Shanghai Institute of Applied Physics, Chinese Academy of Sciences, Shanghai Synchrotron Radiation Facilty (SSRF) Wei, Huibo; Peking University,, College of Chemistry and Molecular Engineering Wang, Z. B.; University of Toronto, Liu, Zhiwei; Peking University, College of Chemistry and Molecular Engineering Bian, Zuqiang; Peking University, College of Chemistry and Molecular Engineering Lu, Zhenghong; University of Toronto, Materials Science and Engineering Zhao, Yongliang; Inner Mongolia University, College of Chemistry and Chemical Engineering Huang, Chunhui; State Key laboratory of Rear Earth Material Chemistry and Applications,

Journal of Materials Chemistry C

Cite this: DOI: 10.1039/c0xx00000x

PAPER

www.rsc.org/xxxxxx

Efficient orange-red phosphorescent organic light-emitting diode using *in situ* synthesized copper(I) complex as the emitter†

Feng Wei,[a,d] Jacky Qiu,[b] Xiaochen Liu,[a] Jianqiang Wang,[c]* Huibo Wei,[a] Zhibin Wang,[b] Zhiwei Liu,[a]* Zuqiang Bian,[a] Zhenghong Lu,[b]* Yongliang Zhao,[d] and Chunhui Huang[a]

Received (in XXX, XXX) Xth XXXXXXXXX 20XX, Accepted Xth XXXXXXXXX 20XX
DOI: 10.1039/b000000x

Inexpensive and eco-friendly luminescent Cu(I) complexes are ideal phosphorescent emitters for high efficiency organic light-emitting diodes (OLEDs). A series of pyrazinyl carbazole (CPz) compounds were designed and synthesized to obtain efficient luminescent Cu(I) complexes through reacting with CuI using vacuum codeposition method. Based on photophysical studies of the CPz compounds and their codeposited CuI:CPz films, the compound 9-(3-(6-(carbazol-9-yl)pyrazin-2-yl)phenyl)-carbazole (CPzPC) with CuI was chosen as the emissive layers for OLED fabrication, where the emitter was identified as $Cu_2(\mu\text{-}I)_2(CPzPC)_4$ on the basis of X-ray absorption spectroscopy. After optimizing the device architecture and material selections including CuI doping concentration and hole transporting layer, efficient orange-red emitting OLEDs with maximum wavelength, external quantum efficiency (EQE) and luminance around 590 nm, 6.6% and 8619 cd m^{-2} (10 V), respectively, was achieved.

Introduction

Organic light-emitting diodes (OLEDs) have been extensively studied due to their potential applications in flat panel or flexible displays and solid state lighting.[1] Phosphorescent OLEDs employing noble transition metal (i.e. iridium and platinum) complexes as emitters have particularly attracted considerable attention due to their ability to harvest both singlet and triplet excitons, leading to a potential internal quantum efficiency of 100%.[2] Unfortunately, the use of noble metal in an OLED greatly increases its cost, presenting a significant barrier to commercialization. So there has been an increasing interest in developing inexpensive materials that can both harvest singlet and triplet energies for use in high-efficiency OLEDs.

Up to now, there are mainly two solutions to reduce the cost of emitters, one is to explore metal-free organic molecules that exhibit efficient thermally activated delayed fluorescence (TADF), in which the energy gap between the singlet and triplet excited states is very small, thereby promoting highly efficient spin up-conversion from non-radiative triplet states to radiative singlet states.[3] The other solution is to develop inexpensive phosphorescent metal complexes, such as Cu(I) complex.[4]

In fact, luminescent Cu(I) complex has been considered as an emitter in OLED simultaneously as iridium complex.[5] However, Cu(I) complex based OLEDs are far fall behind, especially comparing with iridium complex based OLEDs that showing rich colors,[6] high efficiency up to theoretical external quantum efficiency (EQE) of 20%,[7] and long operating lifetimes.[8] This is not because Cu(I) complexes are poor emitters, since several Cu(I) complexes with photoluminescence quantum yield (PLQY) exceed 90% have been reported,[9] but because most Cu(I) complexes are unstable during sublimation and hence not amenable to the vacuum deposition methods typically used to fabricate OLEDs.

Even so, inexpensive and eco-friendly Cu(I) complexes are attractive in OLEDs. By careful design molecular structure, researchers have obtained a few sublimable Cu(I) complexes and fabricated efficient green OLEDs with performance comparable to iridium complexes based ones. For example, Peters *et al*. have obtained a sublimable and highly emissive Cu(I) complex (PLQY = 57%) with tightly bound chelate ligand that can create a rigid environment around the copper center and hence fabricated an efficient green OLED with maximum EQE of 16.1%.[4c] Osawa *et al*. have fabricated even more efficient green OLED with a maximum EQE of 21.3%, by using a sublimable and simple three-coordinate Cu(I) complex as the emitter.[4b]

Bypassing careful design of sublimable Cu(I) complexes for use in OLED, we have demonstrated a codeposition method to make Cu(I) emitters for OLEDs. This method involves codeposition of CuI and pyridine-coordinating ligand/host compound to form Cu(I) complex doped emissive layer *in situ*. With the new device fabrication method, a green OLED showing EQE of 15.7% at a brightness of 100 cd/m^2 was obtained, and the luminescent species was characterized as a halogen-bridged dinuclear complex.[10] The codeposition method is useful to fabricate Cu(I) complex based OLEDs, next comes the question of whether we can tune the emission color and fabricate high efficiency OLEDs other than green.

According to literatures,[4f,9b,11] the electron density in the

highest occupied molecular orbitals (HOMOs) of a halogen-bridged dinuclear Cu(I) complex $Cu_2(\mu\text{-}X)_2L_n$ (X and L are halogen and ligand, respectively, n is the amount of the ligand in the molecule) is distributed over the copper and halogen atoms, while that in the lowest unoccupied molecular orbitals (LUMOs) is localized on the ligands. Thus, the emission color of the *in situ* formed Cu(I) complex could be tuned by varying the electronic structure of the codeposited ligand. Moreover, the codeposited ligand in this case serves a dual role as both a ligand for forming the emissive complex and as a host matrix for the formed emitter, thus the ligand should also be carefully designed to ensure that it is both a good ligand for Cu coordination and a good host matrix for the *in situ* formed Cu(I) complex.

Following aforementioned considerations, three pyrazinyl carbazole (CPz) compounds, 9-(3-(6-(carbazol-9-yl)pyrazin-2-yl)phenyl)-carbazole (CPzPC), 9-(5-(6-(carbazol-9-yl)pyrazin-2-yl)pyridin-3-yl)-carbazole (CPzPyC) and 9-(6-(6-(carbazol-9-yl)pyrazin-2-yl)pyrazin-2-yl)-carbazole (CPzPzC) were designed and synthesized. The pyrazine coordinating unit is mainly designed to realize an red-shifted emission color of the *in situ* formed Cu(I) complex comparing to that of pyridine. The electrical properties of the three CPzs were tuned by varying the central heterocyclic arylene to study the energy transfer status between the CPz ligand and its *in situ* formed Cu(I) complex. After a systematical study of the three CPz compounds and their codeposited CuI:CPz films, it is found that the codeposited CuI:CPzPC film with a molar ratio of 1:7 (corresponding to a CuI doping concentration around 5 wt%) showed the best performance. By adopting the film as the emissive layer and optimizing device architecture and material selection, an orange-red OLED with maximum emission band, EQE, and luminance of 590 nm, 6.6%, and 8619 cd m^{-2}, respectively, were obtained.

Results and discussion

Synthesis and characterization

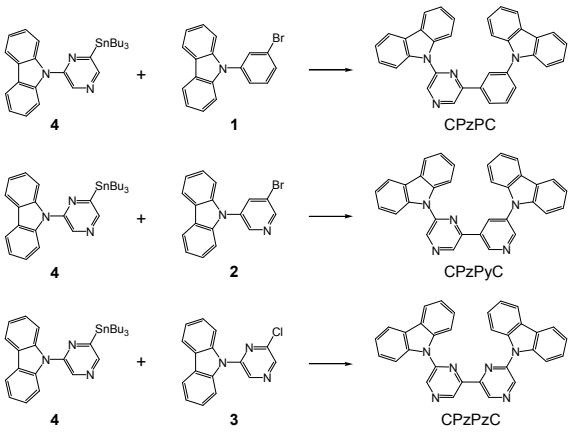

Scheme 1. Synthetic routes to CPzPC, CPzPyC and CPzPzC.

The synthetic routes of the three CPz compounds are depicted in Scheme 1. These compounds were prepared through Stille coupling of an organotin compound 9-(6-(tributylstannyl)pyrazin-2-yl)-carbazole with three halides, purified by simple wash or recrystallization and subsequently twice thermal gradient sublimations. The identification of the three CPz compounds was established on the basis of ^{1}H NMR spectroscopy, mass spectrometry, and elemental analysis. Details are presented in the experimental section.

Photophysical properties

Fig. 1 shows the electronic absorption and photoluminescence (PL) spectra of the three CPz compounds in solution at room temperature. The absorption peaks around 290, 320, and 330 nm can be assigned to the carbazole-centered π–π* transitions, whereas the absorbance at wavelengths longer than 350 nm can be attributed to strong electron affinity of heterocyclic arylene and hence intramolecular charge transfer formed between the central heterocyclic arylene and carbazole,[12] which red-shifts with more nitrogen atoms were added into the heterocyclic arylene. As anticipated, the band gap (E_g) of CPzPzC is 2.8 eV, which is 0.1 eV narrower than that of CPzPyC and CPzPC.

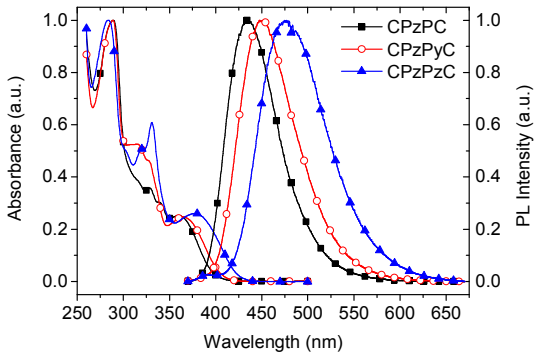

Fig. 1. UV-vis absorption and PL spectra of CPzPC, CPzPyC, and CPzPzC in solution (10^{-5} M).

All the three CPz compounds showed strong blue emission in diluted 2-methyltetrahydrofuran (2-MeTHF) solution, with maximum emission band at 434, 447, and 477 nm for CPzPC, CPzPyC, and CPzPzC, respectively. An obvious red-shift in maximum wavelength is found when introducing more nitrogen atoms in the central heterocyclic arylene. Based on density functional theory (DFT) calculations, the HOMOs of the three CPz compounds are mainly located at the carbazole unit. In contrast, the LUMOs are mainly distributed on the central heterocyclic arylene (Fig. S1 in the Supporting Information). With more nitrogen atoms in the heterocyclic arylene skeleton, the lower laying the LUMO level was obtained (Table S1 in the Supporting Information), which leads to aforementioned red-shift in PL spectrum.

Table 1. The photophysical, electrochemical, and thermal properties of CPzPC, CPzPyC and CPzPzC.

Compd.	λ_{abs} [nm][a]	λ_{em} [nm][b]	E_g [eV][c]	E_T [eV][d]	E_T [eV][e]	HOMO/LUMO [eV][f]	T_g/T_d [°C][g]
CPzPC	288, 329, 341, 364	434	2.9	2.65	2.60	5.9/3.0	96/403
CPzPyC	289, 317, 329, 367	447	2.9	2.65	2.56	6.0/3.1	- /400
CPzPzC	284, 320, 331, 379	477	2.8	-	2.40	6.1/3.3	- /415

[a]Measured in CH_2Cl_2 (10^{-5} M); [b]Measured in 2-MeTHF (10^{-5} M); [c]Calculated from the limit of absorption spectrum; [d]Measured in 2-MeTHF (10^{-5} M) at 77 K; [e]Calculated by Gaussian 03W; [f]HOMO was determined from the oxidation potential, LUMO was deduced from the formula E_g = LUMO – HOMO; [g]Determined by TGA and DSC measurement.

To evaluate the triplet energy (E_T) levels of the CPz compounds, their PL spectra in a frozen 2-MeTHF matrix at 77 K have been examined (Fig. S2 in the Supporting Information). The

compounds CPzPC and CPzPyC showed obvious phosphorescence that distinguishes from their fluorescence transitions, both with the highest energy phosphorescent emission band around 468 nm, corresponding to a E_T of 2.65 eV. Although we failed in estimating the E_T of CPzPzC from its low temperature spectrum, the calculated one is 2.40 eV (Table 1), which is a little lower the those calculated values for CPzPC (2.60 eV) and CPzPyC (2.56 eV).

Electrochemical properties

Cyclic voltammetry was employed to investigate the electrochemical properties of the three CPz compounds and hence to estimate their HOMO/LUMO energy levels. All compounds exhibit irreversible oxidation waves like most carbazole derivatives (Fig. S3 in the Supporting Information).[13] By using ferrocene as an internal/external standard, the oxidation potentials were observed to be 0.9, 1.0 and 1.1 V, thus the HOMO energy levels were estimated to be 5.9, 6.0 and 6.1 eV for CPzPC, CPzPyC and CPzPzC, respectively.[14] Because no clear reduction wave was observed within the potential window of the cyclic voltammogram, the LUMO energy levels were deduced from HOMO energy levels and optical band gaps (i.e. E_g), which are 3.0, 3.1 and 3.3 eV for CPzPC, CPzPyC and CPzPzC, respectively (Table 1).

Thermal properties

The thermal properties of the three CPz compounds were investigated by thermogravimetric analysis (TGA) and differential scanning calorimetry (DSC) (Fig. S4 in the Supporting Information). TGA measurement reveals their high thermal-decomposition temperatures (T_d, corresponding to 5% weight loss) of 403 °C (CPzPC), 400 °C (CPzPyC), and 415 °C (CPzPzC), which are higher than 373 °C of 4,4'-N,N'-dicarbazole-biphenyl (CBP, a widely used host material in OLEDs). During the DSC measurement, only CPzPC exhibits distinct glass-transition temperatures (T_g) of 96 °C during the second heating scan, which is significantly higher than 62 °C of CBP[15] and similar to 95 °C of 1,4-bis[(1-naphythylphenyl)amino]biphenyl (NPB)[16].

Photophysical Properties of Codeposited films

Fig. 2 shows the PL spectra of CPz neat films and a series of CuI:CPz films made by codepositing CuI and CPz in different molar ratios from two separate heating sources in a vacuum chamber. From the spectra, following information can be obtained: First, the CPz compounds showed strong blue emission in thin film, similar as they are in diluted 2-MeTHF solution, while their codeposited CuI:CPz films have dominated orange-red emission that differ markedly from the neat CPz film, implying the formation of phosphorescent Cu(I) complexes.[10] Second, an obvious redshift (~ 30 nm) was found in codeposited CuI:CPz films when the CPz ligand was varied from CPzPC to CPzPyC, and to CPzPzC (i.e. the maximum emission band was observed at 584, 596, and 615 nm for CuI: CPzPC, CuI: CPzPyC, and CuI: CPzPzC, respectively, at a CuI:CPz molar ratio of 1:5), and a slightly blueshift was found when a higher CPz molar ratio was used. The former phenomenon could be attributed to a decreasing molecule energy of the ligand as more nitrogen atoms were added in the central heterocyclic arylene, which lowers the LUMO energy level of the *in situ* formed Cu(I) complex,[11] while the later one may be arised from a lower Cu(I) complex doping concentration that avoiding triplet quenching.

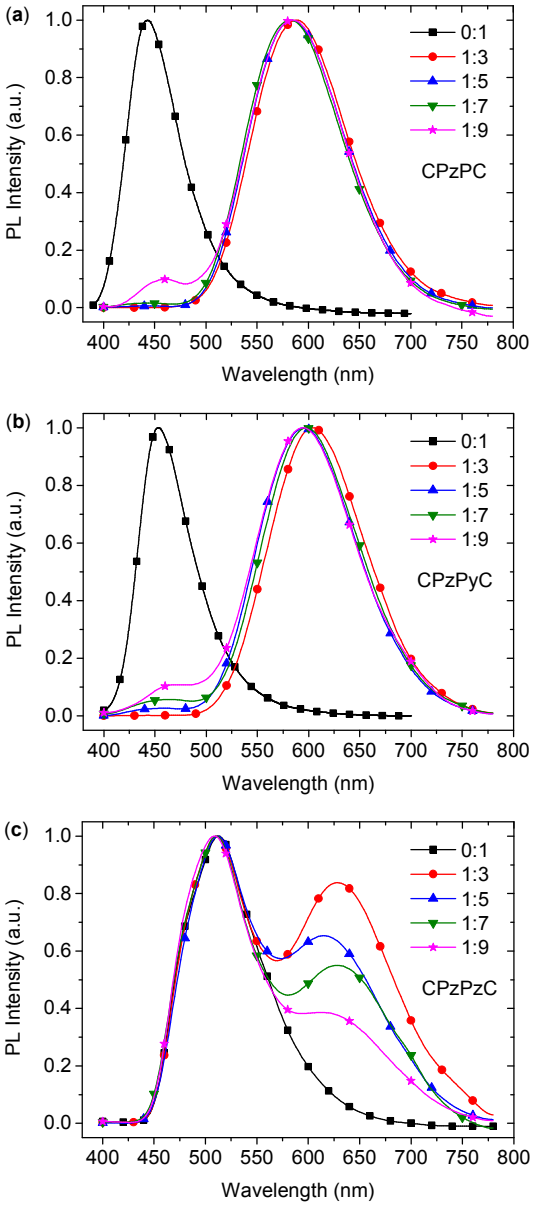

Fig. 2. PL spectra of neat CPz films and codeposited CuI:CPz films with different molar ratios at room temperature, where CPz is a) CPzPC, b) CPzPyC, and c) CPzPzC.

It should be noted that all the CPz compounds have more than one possible coordination sites for CuI to interact with. For example, the compounds CPzPC and CPzPzC have two different nitrogen (N) coordination sites on pyrazinyl, while the compound CPzPyC has a third N coordination site on pyrdinyl. Based on the hard and soft acids and bases theory (HSAB), the Cu^+ cation prefers to interact with pyrazinyl N than pyridinyl N, since Cu^+ cation is a soft acid and pyrazine is a softer base than pyridine. Moreover, the favorable coordination site on pyrazinyl should be the 4-N, due to a severe steric effect of the 1-N. This is in good consistent with the PL studies of the codeposited CuI:CPzPyC films. The CuI:CPzPyC films showed a dominated emission band

that is in line with the CuI: CPzPC and CuI: CPzPzC films, where only coordination between Cu^+ and pyrazinyl N exist. However, it may possible that there are pyridine-coordinating species in the film that showing high energy transition,[10] which can be well transferred to pyrazine-coordinating species, leading to a dominated low energy transition as observed in the PL spectra.

The last but not the least we can deduce from the PL spectra is the energy transfer status between the CPz compound and its *in situ* formed Cu(I) complex. The CPz compound in this case serves a dual role as both a ligand for forming the emissive complex and as a host matrix for the formed emitter. Therefore, whether the CPz based fluorescence was observed could be used as a sign to roughly evaluate the energy transfer status between the CPz compound and its *in situ* formed Cu(I) complex. As shown in the Fig. 2, the codeposited CuI:CPzPC and CuI:CPzPyC films exhibited a very small emissive contribution from the ligand even at high CPz concentrations, while the CuI:CPzPzC films showed an apparent ligand emission even at low CPzPzC concentrations, indicating that the energy transfer between CPzPC or CPzPyC and their corresponding *in situ* formed Cu(I) complex is more efficient than that between CPzPzC and CuI: CPzPzC. As a result, the compounds CPzPC and CpzPyC might be better host materials for their Cu(I) complexes while CPzPzC is definitely not. This is consistent with our PLQY measurement of the three codeposited CuI:CPz films with molar ratio of 1:7 (i.e. CuI doping concentration around 5 wt%), with values of 0.22, 0.17, and 0.04 for CPzPC, CPzPyC, and CPzPzC, respectively.[17]

Chemical Structure in the Codeposited Film

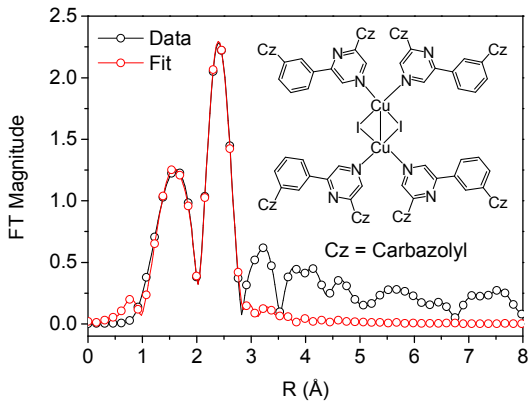

Fig. 3. Fourier transform of the codeposited CuI:CPzPC film with a CuI:CPzPC molar ratio of 1:5 (without phase shift corrected). Inset: Chemical structure of $Cu_2(\mu\text{-}I)_2(CPzPC)_4$.

Table 2. Fit parameters for the codeposited CuI:CPzPC film (CuI:CPzPC = 1:5).

Path	CN[a)]	R [Å][b)]	$\sigma^2\times10^{-3}$[Å^2][c)]
Cu-N	2.0 (fixed)	1.92±0.02	3.8±0.2
Cu-I	1.6±0.3	2.57±0.02	9.3±5.2
Cu-Cu	0.9±0.2	2.61±0.02	14.8±3.9

[a)]Coordination number; [b)]Distance between the Cu atom and surrounding N, I and Cu atoms; [c)]Mean square disorder.

To illustrate the possible chemical structure of the *in situ* synthesized copper(I) complex in film, a codeposited CuI:CPzPC film (molar ratio = 1:5) was measured by X-ray absorption fine structure (XAFS), including X-ray absorption near edge structure (XANES) and extended X-ray absorption fine structure (EXAFS). The XANES analysis (Fig. S5 in the Supporting Information) is similar with our previous codeposited films,[10] confirming the presence of only monovalent Cu in the codeposited film. The Fourier transform of EXAFS fit parameters is listed in Table 2 and Fig. 3. There are three kinds of coordination structure including two Cu-N (1.92±0.02 Å), two Cu-I (2.57±0.02 Å), and one Cu-Cu (2.61±0.02 Å) paths around the Cu(I) center. (The peak at ~1.6 Å is mainly arise from the coordination of Cu-N, while that at ~2.3 Å arises from the coordination layer of Cu-Cu and Cu-I, and the features in the data at R > 3.0 Å are signals from further coordination layer of copper). Thus, the Cu(I) species in the codeposited CuI:CPzPC films is most likely a dimeric complex $Cu_2(\mu\text{-}I)_2(CPzPC)_4$ (Fig. 3, insert).

Electroluminescence Properties

It is well know that high PLQY is an essential factor to fabricate high efficiency OLEDs, herein only the codeposited CuI:CPzPC films were evaluated in OLEDs. With the codeposited emissive layer, our OLEDs has a structure of ITO/ MoO_3 (1 nm)/ hole transport layer (HTL, 35 nm)/ CuI:CPzPC (20 nm)/ 1,3,5-tris(N-phenylbenzimidazole-2-yl)benzene (TPBi, 65 nm)/ LiF (1 nm)/ Al, where the HTL is NPB or CBP (Fig. 4a). The combination of ITO/ MoO_3/ HTL was used as the hole injection media since the thin MoO_3 layer enables direct injection of holes into NPB or CBP, as well as excellent hole transport ability of NPB and CBP. The TPBi layer was used as the electron transport layer because of its proper LUMO energy level and good electron transport ability.

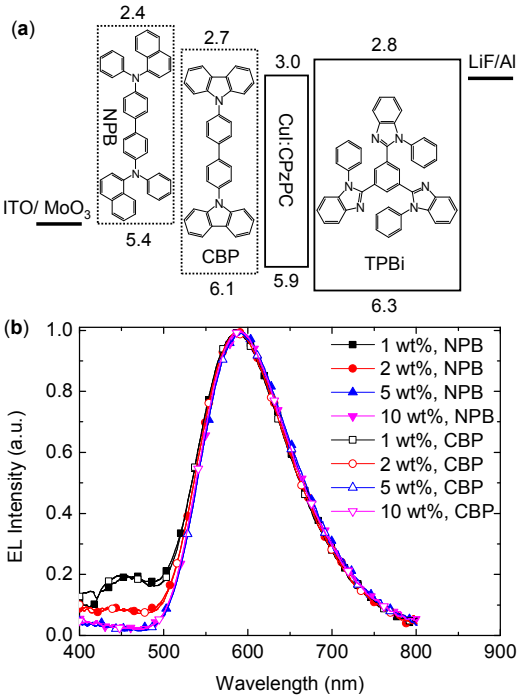

Fig. 4. a) Chemical structure and energy level diagrams of the investigated molecules. b) Electroluminescence spectra of OLEDs **1-8** at an applied voltage of 5 V. The device structure is ITO/ MoO_3 (1 nm)/ HTL (35 nm)/ CuI:CPzPC (*x* wt%, 20 nm)/ TPBi (65 nm)/ LiF (1 nm)/ Al, where the HTL is NPB or CBP, *x* = 1, 2, 5, or 10.

To investigate the effect of CuI doping concentration and HTL

on device performance, eight OLEDs with CuI mass doping concentrations of 1 wt% (devices **1** and **5**), 2 wt% (devices **2** and **6**), 5 wt% (devices **3** and **7**), and 10 wt% (devices **4** and **8**) were fabricated, where the HTL for devices **1**-**4** is NPB, while that for devices **5**-**8** is CBP. Fig. 4b shows electroluminescence (EL) spectra of the devices at 5 V. All devices showed orange-red emission with main peak wavelength around 590 nm that arising from a Cu(I) complex, consistent with the aforementioned PL study. It is found that the EL spectrum of the OLEDs is critical to CuI doping concentration. For example, the devices with high CuI doping concentrations (i.e. 5 wt% and 10 wt%) showed pure EL from the Cu(I) complex, while that with low doping concentrations (i.e. 1 wt% and 2 wt%) exhibited also a small emissive contribution from CPzPC.

Table 3. Performance of OLEDs **1**-**8**.

Device	HTL	CuI conc. [wt%]	V_{on} [a] [V]	L [b] [cd m^{-2}]	PE [c] [lm W^{-1}]	CE [c] [cd A^{-1}]	EQE [c] [%]
1	NPB	1	4.1	4042	4.8/3.5	9.1/5.0	11.8/8.7
2	NPB	2	4.1	4845	5.3/4.1	10.5/6.1	13.6/10.5
3	NPB	5	4.1	5102	5.0/4.3	9.2/5.7	12.1/10.1
4	NPB	10	4.2	4716	4.7/4.2	8.4/5.5	11.4/10.0
5	CBP	1	3.8	6660	4.5/4.2	8.9/6.6	10.8/10.2
6	CBP	2	3.7	7411	5.3/5.0	11.4/8.5	13.5/12.7
7	CBP	5	3.6	8619	6.6/6.3	14.0/10.1	15.9/15.0
8	CBP	10	3.6	8159	6.4/6.2	13.7/10.0	15.6/15.1

[a]V_{on} is the voltage required to reach a brightness of 1 cd m^{-2}; [b]Luminance (L) recorded at 10 V; [c]Data for luminance at 1 and 100 cd m^{-2}, respectively.

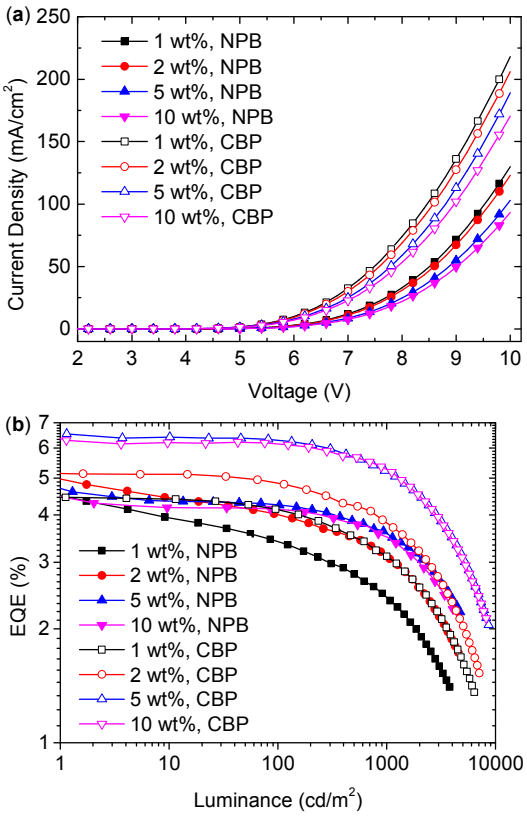

Fig. 5. a) Current density-voltage, and b) EQE-luminance characteristics of OLEDs **1**-**8**.

By comparing the eight OLEDs, it is found that the devices with NPB HTL have lower current density (Fig. 5a), higher driving voltage (Table 3, see also Fig. S6 in the Supporting Information) than these of the devices with CBP HTL, suggests an injection barrier between NPB and CuI:CPzPC layers (0.5 eV for NPB *vs*. 0.1 eV for CBP). Among the OLEDs with the same HTL, the device performance scales with CuI doping concentration (Fig. 5b, see also Fig. S7, S8 in the Supporting Information). For example, the EQE first increases, then decreases with the increasement of the CuI doping concentration (Fig. 4b), which may be arised from a Dexter energy transfer model between emitter and host matrix: at low CuI concentrations (i.e. Cu(I) complex concentrations), the emitter often lies beyond the Dexter transfer radius of an excited CPzPC molecule, while at high concentrations, aggregate quenching is increased.

To summarize the performances of the eight OLEDs (Table 3), the best OLED was obtained with the CBP HTL and an optimal CuI doping concentration of 5 wt%, having peak power efficiency (PE), current efficiency (CE) and EQE of 14.0 lm W^{-1}, 15.9 cd A^{-1} and 6.6%, respectively. At a brightness of 100 cd m^{-2}, a PE of 10.1 lm W^{-1} with an EQE of 6.3% (CE = 15.0 cd A^{-1}) was obtained at an applied voltage of 4.7 V. To our best of knowledge, the performance is among the best OLEDs that using Cu(I) complex as the emitter but with emission colors other than green.[4h,18]

Conclusions

In summary, three pyrazinyl carbazole (CPz) compounds were designed and synthesized to *in situ* codeposition with CuI to form Cu(I) complex doped films, which could be used as the emissive layer in OLEDs. Since these compounds serve a dual role as both a ligand for forming the emissive complex and as a host matrix for the formed emitter, a systematical study was conducted both on the compounds and their codeposited CuI:CPz films, including photophysical properties, electrochemical properties, thermostability, and the possible chemical structure of the *in situ* synthesized copper(I) complex. Consequently, one of the compound CPzPC was selected to be used in OLEDs with a device structure of ITO/ MoO_3 (1 nm)/ HTL (35 nm)/ CuI:CPzPC (20 nm)/ TPBi (65 nm)/ LiF (1 nm)/ Al. By optimizing device architecture and material selection, an orange-red emitting OLED with maximum emission band, EQE, and luminance of 590 nm, 6.6%, and 8619 cd m^{-2} respectively, was achieved. The results demonstrated here implies that codeposition method could be used to fabricate high efficiency Cu(I) complex OLEDs with rich emission colors.

Experimental

General information

Chemicals were received from commercial resource and used as received. ^{1}H-NMR spectrum was recorded on an Bruker-400 MHz NMR spectrometer. Chemical shift data for each signal was reported in ppm units with tetramethylsilane (TMS) as an internal reference, where δ (TMS) = 0. Mass spectra were obtained from a Bruker Apex IV FTMS. Elemental analysis was performed on a vario EL instrument.

Photophysical Measurement

UV-Vis absorption spectra were recorded on a Shimadzu UV-

3100 spectrometer. PL spectra were measured on an Edinburgh Analytical Instruments FLS920 spectrophotometer. PLQY was measured on Nanolog FL3-2iHR spectrometer with a integrating sphere.

Theoretical Calculations

For calculation of HOMO and LUMO energy levels, density functional theory (DFT) calculations were performed for optimized molecular structures and single-point energies at the B3LYP/6-31G(d) and B3LYP/6-311+G(d, p) levels, respectively, using a Gaussian suite of programs (Gaussian 03W). For calculation of ground states (S_0) and triplet excited states (T_1), optimized molecular structures and single-point energies were also calculated at the B3LYP/6-31G(d) and B3LYP/6-311+G(d, p) levels, respectively.

Thermal Properties Measurements

Differential scanning calorimetry was performed on a Q600SDT instrument unit at a heating rate of 15 °C/min from 20 to 300 °C under nitrogen. The glass transition temperature was determined from the second heating scan. Thermogravimetric analysis was undertaken with a Q100DSC instrument. The thermal stability of the samples under a nitrogen atmosphere was determined by measuring their weight loss while heating at a rate of 15 °C/min from 25 to 600 °C.

Cyclic Voltammetry Measurements

Cyclic voltammetry was carried out in nitrogen-purged CH_2Cl_2 solution at room temperature with a CHI600C voltammetric analyser and tetrabutylammonium hexafluorophosphate ($TBAPF_6$) (0.1 M) as the supporting electrolyte. The conventional three-electrode configuration is consists of a platinum working electrode, a platinum wire auxiliary electrode, and an Ag/AgCl wire pseudo-reference electrode.

X-ray Absorption Fine-Structure Measurements

The X-ray absorption data at the Cu K-edge of codeposited CuI:CPzPC film was measured at room temperature in fluorescence mode with an SDD detector at beam line BL14W of the Shanghai Synchrotron Radiation Facility (SSRF), China.

OLED Fabrication and Measurements

All devices were fabricated in a Kurt J. Lesker LUMINOS cluster tool. Commercially patterned indium tin oxide (ITO) anode with a sheet resistance of 15 Ohms sq^{-1} was ultrasonically cleaned with a standard regiment of Alconox, acetone, and methanol followed by UV ozone treatment. Patterned MoO_3 film was thermal vapor deposited on ITO using a shadow mask and treated by *ex situ* oxidation with UV ozone for 30 min. The substrate was then loaded into the cluster tool again to complete the other layers. The organic layers and LiF layer were deposited in a dedicated organic chamber with a base pressure of $\sim 10^{-6}$ Pa. The Al cathode lines (2 mm wide) were deposited orthogonally to the ITO anode lines (1 mm wide) in a separate metallization chamber with a base pressure of $\sim 10^{-5}$ Pa. The current-voltage (*IV*) and luminance measurements were performed using a HP4140B picoammeter and Minolta LS-110 luminance meter in ambient air, respectively.

Syntheses of CPzPzC, CPzPyC and CPzPC

9-(3-bromophenyl)-carbazole (1): A mixture of 1-bromo-3-iodobenzene (30.0 g, 106 mmol), carbazole (17.4 g, 104 mmol), copper powder (20.2 g, 318 mmol), and potassium carbonate (44.0 g, 319 mmol) in DMF (240 mL) was stirred at 130 ºC for 24 hr under nitrogen atmosphere. After cooling to room temperature, the reaction mixture was diluted with ethylacetate and filtered through Celite. The filtrate was poured into water and then extracted with ethylacetate. The combined organic phase was washed with brine and dried over Na_2SO_4. The subjection of the crude mixture to silica gel chromatography (hexane:toluene = 6:1) afforded compound 4 (19.5 g, 58%) as white powder. ^{1}H NMR (400 MHz, $CDCl_3$, δ): 8.15 (s, 1H), 8.13 (s, 1H), 7.75 (t, J = 1.6 Hz, 1H), 7.59-7.61 (m, 1H), 7.52-7.54 (m, 1H), 7.49 (d, J = 7.8 Hz, 1H), 7.40-7.43 (m, 4H), 7.28-7.32 (m, 2H). MS: m/z 322.2.

9-(5-bromopyridin-3-yl)-carbazole (2): A mixture of 3, 5-dibromopyridine (42.6 g, 180 mmol), carbazole (25.0 g, 150 mmol), copper powder (5.0 g, 79 mmol), and potassium carbonate (22.0 g, 160 mmol) in nitrobenzene (250 mL) was stirred at 180 ºC for 24 hr under nitrogen atmosphere. After cooling to room temperature, the reaction mixture was filtered and the residue was washed with dichloromethane. The solvent of the filtrate was removed by distillation at reduced pressure. The residue was purified by column chromatography to yield compound 3 (22.0 g, yield: 45 %) as white powders. ^{1}H NMR (400 MHz, $CDCl_3$, δ): 8.85 (d, J = 1.8 Hz, 1H), 8.79 (d, J = 1.7 Hz, 1H), 8.15 (s, 1H), 8.13 (s, 2H), 7.45 (t, J = 6.0 Hz, 2H), 7.39 (d, J = 7.9 Hz, 2H), 7.34 (t, J = 7.5 Hz, 2H). MS: m/z 323.0.

9-(6-chloropyrazin-2-yl)-carbazole (3): To a stirred mixture of sodium hydride (3.09 g, 70 %, 90 mmol) and anhydrous dimethyl formamide (DMF, 40 mL) was added dropwise carbazole (10.02 g, 60 mmol) in anhydrous DMF (50 mL) at room temperature. After addition, the mixture was stirred at room temperature for 30 min and then cooled to 0 °C, followed by quickly addition of 2,6-dichloropyrazine (10.73 g, 72 mmol) in anhydrous DMF (50 mL). The mixture was allowed to warm to room temperature and stirred for 2.5 h, and then poured into water and the precipitation was collected by filtration. The subjection of the crude mixture to silica gel chromatography (CH_2Cl_2:hexane = 1:5) afforded compound 1 (13.0 g, yield: 77 %) as yellow needle crystals.^{1}H NMR (400 MHz, $CDCl_3$, δ): 8.97 (s, 1H), 8.53 (s, 1H), 8.12 (s, 1H), 8.11 (s, 1H), 7.96 (s, 1H), 7.94 (s, 1H), 7.47-7.52 (m, 2H), 7.39 (t, J = 7.7 Hz, 2H). MS: m/z 280.1.

9-(6-(tributylstannyl)pyrazin-2-yl)-carbazole (4): To a solution of tributyltin hydride (2.4 mL, 9 mmol) in THF (50 mL) at 0 °C was added dropwise LiHMDS (1.0 M solution in THF, 9 mL, 9 mmol). The mixture was stirred at 0 °C for 15 min, at room temperature for 10 min and then cooled to -78 °C, followed by dropwise addition of 9-(6-chloropyrazin-2-yl)-carbazole (2.1 g, 7.5 mmol) in THF (40 mL). The reaction mixture was warmed to room temperature and stirred for 20 h, quenched by satratued NaCl solution and extracted with ether. The combined organic phase was washed with brine and dried over Na_2SO_4. The crude product was purified by column chromatography (hexane:EtOA = 49:1) to yield compound 2 (3.2 g, yiled: 80 %) as a brownish red oil. ^{1}H NMR(400 MHz,$CDCl_3$, δ): 8.82 (s, 1H), 8.52 (s, 1H), 8.13

(s, 1H), 8.11 (s, 1H), 7.91 (s, 1H), 7.89 (s, 1H), 7.43-7.47 (m, 2H), 7.34 (t, J = 7.3 Hz, 2H), 1.60-1.67 (m, 6H), 1.35-1.42 (m, 6H), 1.22-1.26 (m, 6H), 0.88-0.92 (m, 9H). MS: m/z 536.2.

9-(3-(6-(carbazol-9-yl)pyrazin-2-yl)phenyl)-carbazole (CPzPC): To a flask (100 mL) was added compounds **4** (1.34 g, 2.5 mmol), **1** (0.97 g, 3 mmol), $Pd(PPh_3)_4$ (0.09 g, 0.0075 mmol), and toluene (50 mL). The mixture was refluxed for 24 hr under nitrogen atmosphere. After cooling to room temperature, the yellow precipitation was filtered and recrystallized from toluene to obtain a pale yellow solid (0.97 g, yield: 80%), which was further purified by twice thermal gradient sublimation (260 °C- 200 °C- 140 °C) at low pressure (10^{-4} Pa). ^{1}H NMR (400 MHz, $CDCl_3$, δ): 9.06 (d, J = 1.0 Hz, 2H), 8.68-8.69 (m, 2H), 8.55 (d, J = 2.5 Hz, 2H), 8.14 (s, 2H), 8.12 (s, 2H), 7.90 (s, 2H), 7.88 (s, 2H), 7.49 (d, J = 1.1 Hz, 1H), 7.47 (s, 2H), 7.46 (d, J = 1.1 Hz, 1H), 7.35-7.38 (m, 4H). MS: m/z 487.2. Anal. Calc. for $C_{34}H_{22}N_4$: C, 83.93; H, 4.56; N, 11.51. Found: C, 83.82; H, 4.58; N, 11.82.

9-(5-(6-(carbazol-9-yl)pyrazin-2-yl)pyridin-3-yl)-carbazole (CPzPyC): To a flask (250 mL) was added compounds **4** (2.67 g, 5 mmol), **2** (1.94 g, 6 mmol), $Pd(PPh_3)_4$ (0.17g, 0.015mmol), and toluene (100 mL). The mixture was refluxed for 36 hr under nitrogen atmosphere. After cooling to room temperature, the yellow precipitation was filtered and recrystallized from toluene to obtain a pale yellow solid (1.70 g, yield: 70%), which was further purified by twice thermal gradient sublimation (260 °C- 210 °C- 160 °C) at low pressure (10^{-4} Pa). ^{1}H NMR (400 MHz, $CDCl_3$, δ): 9.47 (d, J = 1.9 Hz, 1H), 9.12 (s, 1H), 9.11 (s, 1H), 9.08 (d, J = 2.3 Hz, 1H), 8.77 (t, J = 2.1 Hz, 1H), 8.18 (s, 1H), 8.16 (s, 1H), 8.14 (s, 1H), 8.12 (s, 1H), 8.03 (s, 1H), 8.01 (s, 1H), 7.54 (s, 1H), 7.52 (s, 1H), 7.44-7.49 (m, 4H), 7.38-7.40 (m, 4H). MS: m/z 488.2. Anal. Calcd. for $C_{33}H_{21}N_5$: C, 81.29; H, 4.34; N, 14.36. Found: C, 81.12; H, 4.35; N, 14.49.

9-(6-(6-(carbazol-9-yl)pyrazin-2-yl)pyrazin-2-yl)-carbazole (CPzPzC): To a flask (250 mL) was added compounds **4** (2.67 g, 5 mmol), **3** (1.68 g, 6 mmol), $Pd(PPh_3)_4$ (0.17 g, 0.015 mmol), and toluene (100 mL). The mixture was refluxed for 20 hr under nitrogen atmosphere. After cooling to room temperature, the yellow precipitation was filtered and washed with petroleum ether. The compound CPzPzC was further purified by thermal gradient sublimation (280 °C- 230 °C- 180 °C) at low pressure (10^{-4} Pa) twice to yield yellow solid (1.20 g , yield: 49%). ^{1}H NMR (400 MHz, $CDCl_3$, δ): 9.64 (s, 2H), 9.21 (s, 2H), 8.19 (s, 2H), 8.17 (s, 2H), 8.08 (s, 2H), 8.06 (s, 2H), 7.56-7.52 (m, 4H), 7.45-7.41 (m, 4H). MS: m/z 489.2.Anal. Calcd. for $C_{32}H_{20}N_6$: C,78.67; H,4.13; N,17.20. Found: C,78.67; H,4.12; N,17.26.

Acknowledgment

We greatly acknowledge the financial support by The National Basic Research Program of China (No. 2006CB601103), The National Natural Science Foundation of China (NNSFC, Nos. 20971006, 90922004, 21201011, 91127001), and The Specialized Research Fund for the Doctoral Program of Higher Education (20120001120116).

Notes and references

[a]*Beijing National Laboratory for Molecular Sciences (BNLMS), State Key Laboratory of Rare Earth Materials Chemistry and Applications, College of Chemistry and Molecular Engineering, Peking University, Beijing 100 871, P. R. China. E-mails: zwliu@pku.edu.cn; Fax: (+86) 10-6275-4745. Tel: (+86) 10-6275-7156.*

[b]*Department of Materials Science and Engineering, University of Toronto, 184 College Street, Toronto, Ontario, Canada M5S 3E4. E-mail: zhenghong.lu@utoronto.ca.*

[c]*Shanghai Institute of Applied Physics, Chinese Academy of Sciences, Shanghai 201204, P. R. China. E-mail: wangjianqiang@sinap.ac.cn*

[d]*College of Chemistry and Chemical Engineering, Inner Mongolia University, Hohhot 010021, P. R. China*

†Electronic Supplementary Information (ESI) available: DFT caculations (Fig. S1, Table S1), low temperature PL spectra (Fig. S2), cyclic voltammetry curves (Fig. S3), thermogravimetric analysis and differential scanning calorimetry curves (Fig. S4) of CPzPC, CPzPyC, and CPzPzC, Cu K-edge of the codeposited CuI:CPzPC film (Fig.S5), and luminance-voltage (Fig. S6), power efficiency-luminance (Fig. S7), and current efficiency-luminance (Fig. S8) characteristics of OLEDs **1**-**8**. See DOI: 10.1039/b000000x/.

1 (*a*) C. W. Tang and S. A. Vanslyke, *Appl. Phys. Lett.*, 1987, **51**, 913; (*b*) S. Reineke, F. Lindner, G. Schwartz, N. Seidler, K. Walzer, B. Lussem and K. Leo, *Nature*, 2009, **459**, 234.

2 (*a*) M. A. Baldo, D. F. O'Brien, Y. You, A. Shoustikov, S. Sibley, M. E. Thompson and S. R. Forrest, *Nature*, 1998, **395**, 151; (*b*) M. A. Baldo, S. Lamansky, P. E. Burrows, M. E. Thompson and S. R. Forrest, *Appl. Phys. Lett.,* 1999, 75, 4; (*c*) Y. G. Ma, H. Y. Zhang, J. C. Shen and C. M. Che, *Synthetic Met.*, 1998, **94**, 245; (*d*) A. R. G. Smith, J. L. Ruggles, H. Cavaye, P. E. Shaw, T. A. Darwish, M. James, I. R. Gentle and P. L. Burn, *Adv. Funct. Mater.*, 2011, **21**, 2225; (*e*) T. C. Lee, J. Y. Hung, Y. Chi, Y. M. Cheng, G. H. Lee, P. T. Chou, C. C. Chen, C. H. Chang and C. C. Wu, *Adv. Funct. Mater.*, 2009, **19**, 2639; (*f*) C. L. Ho, W. Y. Wong, Q. Wang, D. G. Ma, L. X. Wang and Z. Y. Lin, *Adv. Funct. Mater.*, 2008, **18**, 928; (*g*) B. W. Ma, P. I. Djurovich, S. Garon, B. Alleyne and M. E. Thompson, *Adv. Funct. Mater.*, 2006, **16**, 2438; (*h*) J. Q. Ding, J. Gao, Y. X. Cheng, Z. Y. Xie, L. X. Wang, D. G. Ma, X. B. Jing and F. S. Wang, *Adv. Funct. Mater.*, 2006, **16**, 575; (*i*) A. Tsuboyama, H. Iwawaki, M. Furugori, T. Mukaide, J. Kamatani, S. Igawa, T. Moriyama, S. Miura, T. Takiguchi, S. Okada, M. Hoshino and K. Ueno, *J. Am. Chem. Soc.*, 2003, **125**, 12971; (*j*) C. Cebrian, M. Mauro, D. Kourkoulos, P. Mercandelli, D. Hertel, K. Meerholz, C. A. Strassert and L. De Cola, *Adv. Mater.*, 2013, **25**, 437; (*k*) B. W. D'Andrade, J. Brooks, V. Adamovich, M. E. Thompson and S. R. Forrest, *Adv. Mater.*, 2002, **14**, 1032.

3 (*a*) Q. S. Zhang, J. Li, K. Shizu, S. P. Huang, S. Hirata, H. Miyazaki and C. Adachi, *J. Am. Chem. Soc.*, 2012, **134**, 14706; (*b*) T. Nakagawa, S. Y. Ku, K. T. Wong and C. Adachi, *Chem. Commun.*, 2012, **48**, 9580; (*c*) G. Mehes, H. Nomura and Q. S. Zhang, T. Nakagawa and C. Adachi, *Angew Chem. Int. Edit.*, 2012, **51**, 11311; (*d*) S. Y. Lee, T. Yasuda, H. Nomura and C. Adachi, *Appl. Phys. Lett.*, 2012, **101**, 093306; (*e*) A. Endo, M. Ogasawara, A. Takahashi, D. Yokoyama, Y. Kato and C. Adachi, *Adv. Mater.*, 2009, 21, 4802; (*f*) A. Endo, K. Sato, K. Yoshimura, T. Kai, A. Kawada, H. Miyazaki and C. Adachi, *Appl. Phys. Lett.*, 2011, **98**, 083302; (*g*) H. Uoyama, K. Goushi, K. Shizu, H. Nomura and C. Adachi, *Nature*, 2012, **492**, 234.

4 (*a*) Q. S. Zhang, T. Komino, S. P. Huang, S. Matsunami, K. Goushi and C. Adachi, *Adv. Funct. Mater.*, 2012, **22**, 2327; (*b*) M. Hashimoto, S. Igawa, M. Yashima, I. Kawata, M. Hoshino and M. Osawa, *J. Am. Chem. Soc.*, 2011, **133**, 10348; (*c*) J. C. Deaton, S. C. Switalski, D. Y. Kondakov, R. H. Young, T. D. Pawlik, D. J. Giesen, S. B. Harkins, A. J. M. Miller, S. F. Mickenberg and J. C. Peters, *J. Am. Chem. Soc.*, 2010, **132**, 9499; (*d*) L. Zhang, B. Li and Z. Su, *J. Phys. Chem. C*, 2009, **113**, 13968; (*e*) Q. Zhang, J. Ding, Y. Cheng, L. Wang, Z. Xie, X. Jing and F. Wang, *Adv. Funct. Mater.*, 2007, **17**, 2983; (*f*) A. Tsuboyama, K. Kuge, M. Furugori, S. Okada, M. Hoshino and K. Ueno, *Inorg. Chem.*, 2007, **46**, 1992; (*g*) Q. S. Zhang, Q. G. Zhou, Y. X. Cheng, L. X. Wang, D. G. Ma, X. B. Jing and F. S. Wang, *Adv. Funct. Mater.*, 2006, **16**, 1203; (*h*) G. Che, Z. Su, W. Li, B. Chu, M. Li, Z. Hu and Z. Zhang, *Appl. Phys. Lett.*, 2006, **89**, 103511; (*i*) Q. S. Zhang, Q. G. Zhou, Y. X. Cheng, L. X.

Wang, D. G. Ma, X. B. Jing and F. S. Wang, *Adv. Mater.*, 2004, **16**, 432; (*j*) M. Noto, Y. Goto and M. Era, *Chem. Lett.*, 2003, **32**, 32.
5 Y. G. Ma, C. M. Che, H. Y. Chao, X. M. Zhou, W. H. Chan and J. C. Shen, *Adv. Mater.*, 1999, **11**, 852.
6 S. Lamansky, P. Djurovich, D. Murphy, F. Abdel-Razzaq, H. E. Lee, C. Adachi, P. E. Burrows, S. R. Forrest and M. E. Thompson, *J. Am. Chem. Soc.*, 2001, **123**, 4304.
7 (*a*) Z. B. Wang, M. G. Helander, J. Qiu, D. P. Puzzo, M. T. Greiner, Z. W. Liu and Z. H. Lu, *Appl. Phys. Lett.*, 2011, **98**, 073310; (*b*) M. G. Helander, Z. B. Wang, J. Qiu, M. T. Greiner, D. P. Puzzo, Z. W. Liu and Z. H. Lu, *Science*, 2011, **332**, 944; (*c*) G. F. He, M. Pfeiffer, K. Leo, M. Hofmann, J. Birnstock, R. Pudzich and J. Salbeck, *Appl. Phys. Lett.*, 2004, **85**, 3911.
8 E. Orselli, J. Maunoury, D. Bascour and J. P. Catinat, *Org. Electron.*, 2012, **13**, 1506.
9 (*a*) R. Czerwieniec, J. B. Yu and H. Yersin, *Inorg. Chem.*, 2011, **50**, 8293; (*b*) D. M. Zink, M. Bachle, T. Baumann, M. Nieger, M. Kuhn, C. Wang, W. Klopper, U. Monkowius, T. Hofbeck, H. Yersin and S. Brase, *Inorg. Chem.*, 2013, **52**, 2292.
10 (a) Z. W. Liu, M. F. Qayyum, C. Wu, M. T. Whited, P. I. Djurovich, K. O. Hodgson, B. Hedman, E. I. Solomon and M. E. Thompson, *J. Am. Chem. Soc.*, 2011, **133**, 3700; (b) Z. W. Liu, J. Qiu, F. Wei, J. Q. Wang, X. C. Liu, M. G. Helander, S. Rodney, Z. B. Wang, Z. Q. Bian, Z. H. Lu, M. E. Thompson, and C. H. Huang, *Chem. Mater.*, 2014, **26**, 2368.
11 H. Araki, K. Tsuge, Y. Sasaki, S. Ishizaka and N. Kitamura, *Inorg. Chem.*, 2005, **44**, 9667.
12 S. J. Su, C. Cai and J. Kido, *Chem. Mater.*, 2011, **23**, 274.
13 G. Zotti, G. Schiavon, S. Zecchin, J. F. Morin and M. Leclerc, *Macromolecules*, 2002, **35**, 2122.
14 B. W. D'Andrade, S. Datta, S. R. Forrest, P. Djurovich, E. Polikarpov and M. E. Thompson, *Org. Electron.*, 2005, **6**, 11.
15 M. H. Tsai, Y. H. Hong, C. H. Chang, H. C. Su, C. C. Wu, A. Matoliukstyte, J. Simokaitiene, S. Grigalevicius, J. V. Grazulevicius and C. P. Hsu, *Adv. Mater.*, 2007, **19**, 862.
16 J. N. Moorthy, P. Venkatakrishnan, D. F. Huang and T. J. Chow, *Chem. Commun.*, 2008, **18**, 2146.
17 We found that the codeposited CuI:CPz films are very sensitive to oxygen, thus the reported PLQY values may lower than their true values because they are measured under air as quickly as possible due to the limitation of our instrument.
18 J. H. Min, Q. S. Zhang, W. Sun, Y. X. Cheng and L. X. Wang, *Dalton Trans.*, 2011, **40**, 686.

Graphics for Contents

Efficient orange-red phosphorescent organic light-emitting diode using *in situ* synthesized copper(I) complex as the emitter

Feng Wei, Jacky Qiu, Xiaochen Liu, Jianqiang Wang,* Huibo Wei, Zhibin Wang, Zhiwei Liu,* Zuqiang Bian, Zhenghong Lu,* Yongliang Zhao, and Chunhui Huang

Orange-red phosphorescent organic light-emitting diodes with inexpensive and eco-friendly luminescent Cu(I) complexes as the emitter are successfully realized by codeposition of copper iodide (CuI) and 9-(3-(6-(carbazol-9-yl)pyrazin-2-yl)phenyl)-carbazole (CPzPC) as the emissive layer, which was chosen in OLED fabrication after a systematical photophysical study of three pyrizly carbazole (CPz) compounds and their codeposited CuI:CPz films.